



A Fourier-Based Comparative Analysis of Discrete 3D Laplacians for Isotropy

Sohail Ahmed Memon

Department of Mathematics, Shah Abdul Latif University, Khairpur Mirs

Email: suhail.memon@salu.edu.pk

Israr Ahmed

Department of Mathematics, Shah Abdul Latif University, Khairpur Mirs

Email: israr.memon@salu.edu.pk

Darshan Mal

Department of Mathematics, Shah Abdul Latif University, Khairpur Mirs

Email: darshan.lal@salu.edu.pk

Imtiaz Ahmed

Department of Mathematics, Shah Abdul Latif University, Khairpur Mirs

Email: sharimtia2014@gmail.com

Abstract

An elliptic partial differential operator, well known as Laplacian operator has diversified applications in fields of science. Its applications comprise numerical analysis, heat flow equations, polymers, image processing, etc. Our work presents the study of three-dimensional discrete Laplacian operators, their formulations in finite difference schemes to analyse their Isotropies and Fourier Stabilities. A few number of three-dimensional Laplacians have been chosen based on different stencil size which are comprised of 7-point, 15-point, 19-point and a family of 27-point. This research study focuses on the mathematical formulation of 3D Laplacian operators, especially to carry out its finite difference for the best stencil identification to be isotropic and to avoid anomalies (artefacts). Using discrete Fourier analysis, we derive the modified wavenumber symbols for each scheme and evaluate their isotropy and dispersion characteristics. The analysis reveals the directional accuracy and stability properties of these Laplacians, which are critical in numerical solutions of elliptic and parabolic partial differential equations (PDEs) in three dimensions. The surface contours plots show a visual comparison of isotropic behaviour of each Laplacian with ideal Laplacian. The 27-point stencils have achieved improved isotropy which can be used in the simulations of 3D heat diffusion equation, cell dynamical model (CDS) and hydrodynamics lattice. Future work includes the derivations of 3D Laplacians for adaptive grids or irregular domains.

Keywords: Discrete 3D Laplacian; Isotropy Analysis; 3D Stencil Operators; Fourier Method

1. Introduction

The Laplacian operator is a fundamental mathematical tool widely used in modelling physical phenomena such as diffusion, heat transfer, electrostatics, quantum mechanics, and fluid dynamics. Its accurate numerical discretization is crucial in solving partial differential equations (PDEs),



Vol. 3 No. 6 (June) (2025)

especially in three-dimensional computational domains.

Mathematically, the partial differential operator (Laplacian) can be represented as [1]:

$$\nabla \cdot \nabla(\psi) = \sum_{i=1}^N \frac{\partial^2 \psi}{\partial x_i^2}, \quad x_i = x, y, z \text{ dimensions} \quad (1)$$

The isotropy is among the essential requirements in discrete Laplacian design. The isotropy is defined as the ability to preserve rotational symmetry in all directions. Discretization schemes that lack isotropy can introduce directional artifacts and numerical anisotropy, degrading simulation accuracy in problems where physical processes are inherently isotropic [1, 2].

To address this challenge, various finite difference schemes for discretization of the 3D Laplacian have been proposed, each offering trade-offs between computational efficiency, accuracy, and isotropic behaviour. In this work, we analyse and compare the commonly used Laplacian stencils consisting 7-point, 15-point, 19-point, and 27-point schemes. These stencils differ in the number and spatial arrangement of the grid points they incorporate, affecting their spectral properties and directional accuracy [4]. Using discrete Fourier analysis, we derive and compare the Fourier symbols of each scheme to quantify their deviation from the ideal continuous Laplacian, particularly in the low-wavenumber regime, where isotropy is most critical.

The discrete Laplacians are implemented in central difference schemes (CDS) and tested through their Fourier modes as numerical simulations. Although stability is a critical aspect of numerical schemes, this study focuses primarily on the spatial characteristics of the Laplacian operators, and does not address time step constraints under explicit integration.

Through comparative visualizations, we highlight the isotropic strengths and weaknesses of each stencil. The isotropy behaviour observed in our extended 3D Laplacian schemes is consistent with improved symmetry properties presented in the work of Shinozaki and Oono [1], [5], [6] which is a contextual support for our findings.

This work contributes to the understanding of stencil-based Laplacian discretization in 3D by offering spectral evidence for choosing an appropriate scheme based on application needs such as computational physics, image processing, and 3D reaction-diffusion modelling [7].

The mathematical sciences are evolving rapidly and the Laplacians become more and more applicable in many scientific soft fields. Therefore, the isotropy of the 3D Laplacians need to be explored in terms of anisotropy and stability considerations.

Many researchers have conducted studies to investigate the isotropy of 3D Laplacians but no any specified method of quantification of isotropy for Laplacian operator has been reported properly. In this study, we have incorporated isotropy quantification techniques for 3D Laplacians and have suggested the optimal isotropy for chosen 3D Laplacians.

In section 2, the literature review is presented that highlights the applications of 3D Laplacians. Section 3 presents the mathematical formulation of 3D Laplacians. Section 4 is about the stability analysis comprising Fourier equations of 3D Laplacians. Isotropic visualization through surface contour plots of 3D Laplacians are presented in section 5 and finally conclusions are given in section 6.

2. Literature Review

The Laplacian operator is a partial differential operator represented as the divergence of the



Vol. 3 No. 6 (June) (2025)

gradient of a function on Euclidean space. It was first implemented during mid 18th century by a French Mathematician Pierre-Simon de Laplace [8] in a work on celestial mechanics related to moving objects in space. The ability of Laplacian operator to approximate the second-order derivatives makes it vital in solving partial differential equations (PDEs) in many scientific fields, either linear or non-linear. The PDEs describe physical phenomena across spatial domains which comprise computational physics, fluid dynamics, wave propagation, quantum physics, biomedical modelling, image processing (edge detection), flux density of a function's gradient flow and spectral clustering applications [9]. The literature review covers the applications where discretized 3D Laplacians are implemented.

The discretized 3D Laplacians were earlier used in the numerical solution of parabolic and elliptical PDEs including Laplace, Poisson and heat equations [2], [3]. Such equations often emerge in modelling steady-state, electrostatic potentials, transient heat conduction and fluid pressure fields. The fundamental 7-point stencil, that engages nearest neighbours in a 3D grid, has been widely applied for its computational efficiency [10]. Although, the operator using 7-point stencil is treated anisotropic that hinders isotropy by striking artifacts or errors in simulations. To deal these issues of isotropy, the stencils in bigger sizes comprising 15-point, 19-point and 27 point Laplacians have been worked out [4], [11]. The experiments have shown that higher-order operators based on large stencils decrease directional bias and obtain optimal accuracy in simulations of wave propagation and electromagnetic field [12], [13]. In computational electromagnetics, to approximate the spatial derivatives is indispensable for the solution of Maxwell's equations using finite difference time-domain (FDTD) approaches [14].

The discretization of 3D Laplacians are widely implemented in computational fluid dynamics (CFD) and phase field modelling. In CFD, the solution of Navier-Stocks and vorticity transport equations is carried out. Also, in turbulence modelling and incompressible flow solvers where the pressure Poisson equation is a computational challenge, such solution incorporates the discretized Laplacians [15]. Relatedly, the simulation of phase separation, solidification, or crystal growth in phase field models are governed by the Laplacians for interface evolution and curvature effects [16]. Discretised Laplacians were used in three-dimensional simulations of spinodal decomposition by Shinozaki and Oono where stencil selection was thought important for preserving isotropic domain growth. Their research highlighted how the artifacts or anisotropy affected the physical evolution of interfaces in coarsening systems [1], [17].

Image processing is a vast field where 3D Laplacian are utilized extensively. Various simulations are performed in the subfields of image processing, specifically in computer vision and medical high dimensional images. The discretized Laplacians play a vital role in feature enhancement, edge detection and de-noising in image data [18], [19]. The Laplacian of Gaussian, anisotropic diffusion and volume segmentation are the techniques which use accurate and isotropic discretized equations of these for approximations of spatial derivatives.

A work based on anisotropic diffusion in image processing was conducted by Weickert which emerged as pioneering for utilizing discretised three-dimensional Laplacians in the system preserving for smoothness and medical volume enhancement [20]. The discretised 3D Laplacians have proved backbone in regularization and stabilization of inverse problems for improving the quality of images and noise suppression in the fields of tomography and 3D construction [21].

Geophysical simulations is another exciting area where discretized three-dimensional are implemented which include underground fluid transport and modelling seismic wave propagation [22]. Also, the biomedical engineering implements these operators where they are used in



Vol. 3 No. 6 (June) (2025)

simulations of drug dispersion, diffusion of ions, and neutral signal propagation in three-dimensional grids for anatomical structures [23]. No doubt, such big applications require high numerical stability and reliability and motive to work on extended sized stencils of 19-point and 27-point for better isotropy.

Thampi et al. [24] has given a stronger presentation for the discretised Laplacians on a hybrid Lattice Boltzmann frameworks, demonstrating isotropic stencil on grids for accurate interface dynamics. They have mostly used the schemes based on bigger sized stencils such as 15-point, 19-point, and 27-point to overcome the isotropy. Also, they have incorporated the well-designed approach for the comparisons various schemes in 2D and 3D for isotropy and for reduced directional bias. Such isotropic Laplacians have applications in cell-dynamical simulations where rotational symmetry is a key factor [25].

Isotropic discrete Laplacians are considered significant for accurate modelling in phase separation and fluid flow. In this connection, the recent works have been implemented with algebraic methods that derive isotropic Laplacians by averaging functions on discrete spherical surfaces [20]. After the successful implementation of these methods by lattice hydrodynamics, discretised Laplacians are then connected to the Maxwell-Boltzmann equilibrium distribution which provide a strategy to construct isotropic stencils comprising suitable stencils such as 15 points in three dimensions [26]. Latest research has been dedicated on analysing properties of isotropy on different stencils for three-dimensional discretized Laplacians using Fourier or von Neumann stability analysis [4], [27]. These investigations are important for understanding the dispersion and stability analysis of numerical schemes. The better isotropic Laplacians offer optimal accuracy in three-dimensional simulations based on waves, geometric flows and diffusive processes.

Comparative analysis of three-dimensional Laplacians shows that if 7-point based stencil is anisotropic, how do 15-point, 19-point and 27-point exhibit better isotropy and yield improved results in simulations sensitive to directional bias.

3. Discrete Three-dimensional (3D) Laplacian Operators

The construction and mathematical formulation of three-dimensional Laplacian operators are presented in this section. The schemes include 7-point, 15-point, 19-point and 27-point based stencils, leading into their spectral analysis in subsequent sections.

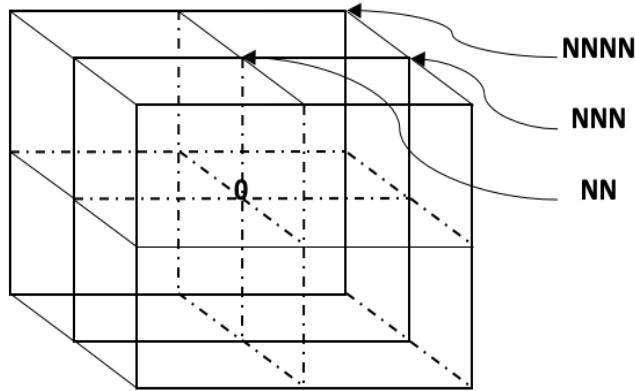


Figure 1. Three-dimensional grid with centre at point O . The NN, NNN and NNNN represent nearest neighbours, next-nearest neighbours and next next-nearest neighbour.

A three-dimensional grid is shown in Figure 1, the first layer is comprised of nearest neighbouring points. Second layer is laid on next nearest neighbouring points and the third layer contains next next-nearest neighbouring points. The finite difference schemes for various stencils based Laplacians are derived through finite difference methods considering NN, NNN or NNNNs. For example, the 7-point Laplacian scheme involve NN points.

The Laplacian scheme for 7-point stencil, given in equation (2), is the fundamental finite difference approximation in the family of 3D Laplacian operators on a uniform Cartesian grid. The scalar field $\psi_{i,j,k}$ is defined on a discrete grid with h space in each direction. The points on the grid are taken in x, y and z directions denoted by i, j and k .

$$\Delta(\psi_{i,j,k}) = \frac{1}{h^2} (\psi_{i+1,j,k} + \psi_{i-1,j,k} + \psi_{i,j+1,k} + \psi_{i,j-1,k} + \psi_{i,j,k+1} + \psi_{i,j,k-1}) \quad (2)$$

The equation (2) is formulated more compactly in equation (3).

$$\Delta(\psi)_{D3Q7} = \frac{1}{h^2} \left[\sum_{i=1}^6 \psi^{(1)} - 6\psi^{(0)} \right], \quad (3)$$

The notation $D3Q7$ in equation (3) is representing the stencil based on 7 neighbouring points in three dimensions. The notation $\psi^{(1)}$ in equation (3) calculates values the immediate 6 neighbours (NN) in $\pm x, \pm y$ and $\pm z$ directions from the centre point. The 7-point stencil engages only nearest neighbours and therefore it is thought computationally efficient but less isotropic particularly in the problems where directional behaviour is highly important [28].

The finite difference approximation schemes for 3D Laplacians based on 15-point, 19-point and 27-point are given in equations (4), (5) and (6) which have been formed involving points from next-nearest neighbours and next next-nearest neighbours from centre point. The 15-point, 19-point and 27-point 3D Laplacians are discussed in literature as isotropic [4], [28].



$$\Delta(\psi)_{D3Q15} = \frac{1}{12h^2} \left[8 \sum_{i=1}^6 \psi^{(1)} + \sum_{i=1}^8 \psi^{(2)} - 56\psi^{(0)} \right] \quad (4)$$

$$\Delta(\psi)_{D3Q19} = \frac{1}{6h^2} \left[2 \sum_{i=1}^6 \psi^{(1)} + \sum_{i=1}^{12} \psi^{(2)} - 24\psi^{(0)} \right] \quad (5)$$

$$\Delta(\psi)_{D3Q27} = \frac{1}{36h^2} \left[16 \sum_{i=1}^6 \psi^{(1)} + 4 \sum_{i=1}^{12} \psi^{(2)} + \sum_{i=1}^8 \psi^{(3)} - 152\psi^{(0)} \right] \quad (6)$$

$$\Delta(\psi)_{PK-D3Q27} = \frac{1}{30h^2} \left[14 \sum_{i=1}^6 \psi^{(1)} + 3 \sum_{i=1}^{12} \psi^{(2)} + \sum_{i=1}^8 \psi^{(3)} - 128\psi^{(0)} \right] \quad (7)$$

$$\Delta(\psi)_{SO-D3Q27} = \frac{1}{22h^2} \left[6 \sum_{i=1}^6 \psi^{(1)} + 3 \sum_{i=1}^{12} \psi^{(2)} + \sum_{i=1}^8 \psi^{(3)} - 80\psi^{(0)} \right] \quad (8)$$

Patra and Karttunen have given different weights for the 27-point Laplacian scheme, given in equation (7) [4]. Shinozaki and Oono have used equation (8) in CDS and this scheme is isotropic but not the optimal choice for achieving isotropy [29]. The equations (6) and (7) are shown isotropic at the quartic order and equation (8) is shown not being isotropic at the quartic order [28]. The subscripts $PK - D3Q27$ and $SO - D3Q27$ in equations (7) and (8) show that the schemes were introduced by Patra and Karttunen (PK) and Shinozaki and Oono (SO).

4. Stability Analysis

The analysis of numerical stability of the discretized Laplacians schemes using Fourier (von Neumann) is presented in this section. It is implemented to analyse the stability of finite difference schemes for various partial differential equations. The main objective is to determine isotropy of each stencil based Laplacian.

The discrete Laplacian operator Δ_h applied to a result in multiplication by Fourier symbol $\Gamma(k)$ which has basis on spatial wave number $k = (k_x, k_y, k_z)$. The discretised three-dimensional Laplacians are implemented in Fourier domain which are follows:

$$\Gamma(k)_{D3Q7} = \frac{2}{(\Delta x)^2} [\cos(k_x \Delta x) + \cos(k_y \Delta x) + \cos(k_z \Delta x) - 3] \quad (9)$$

$$\Gamma(k)_{D3Q15} = \frac{1}{6(\Delta x)^2} \left[8(\cos(k_x \Delta x) + \cos(k_y \Delta x) + \cos(k_z \Delta x)) + 4(\cos(k_x \Delta x) \cos(k_y \Delta x) \cos(k_z \Delta x)) - 28 \right] \quad (10)$$



$$\begin{aligned} & \Gamma(k)_{D3Q19} \\ &= \frac{1}{3(\Delta x)^2} \left[\begin{aligned} & 2(\cos(k_x \Delta x) + \cos(k_y \Delta x) + \cos(k_z \Delta x)) \\ & + 4 \left(\begin{aligned} & \cos(k_x \Delta x) \cos(k_y \Delta x) + \cos(k_x \Delta x) \cos(k_z \Delta x) \\ & \cos(k_y \Delta x) \cos(k_z \Delta x) \end{aligned} \right) - 12 \end{aligned} \right] \quad (11) \end{aligned}$$

$$\begin{aligned} & \Gamma(k)_{D3Q27} \\ &= \frac{1}{9(\Delta x)^2} \left[\begin{aligned} & 8(\cos(k_x \Delta x) + \cos(k_y \Delta x) + \cos(k_z \Delta x)) \\ & + 4 \left(\begin{aligned} & \cos(k_x \Delta x) \cos(k_y \Delta x) + \cos(k_x \Delta x) \cos(k_z \Delta x) \\ & + \cos(k_y \Delta x) \cos(k_z \Delta x) \end{aligned} \right) \\ & + 2(\cos(k_x \Delta x) \cos(k_y \Delta x) \cos(k_z \Delta x)) - 38 \end{aligned} \right] \quad (12) \end{aligned}$$

$$\begin{aligned} & \Gamma(k)_{PK-D3Q27} \\ &= \frac{1}{15(\Delta x)^2} \left[\begin{aligned} & 14(\cos(k_x \Delta x) + \cos(k_y \Delta x) + \cos(k_z \Delta x)) \\ & + 6 \left(\begin{aligned} & \cos(k_x \Delta x) \cos(k_y \Delta x) + \cos(k_x \Delta x) \cos(k_z \Delta x) \\ & + \cos(k_y \Delta x) \cos(k_z \Delta x) \end{aligned} \right) \\ & + 4(\cos(k_x \Delta x) \cos(k_y \Delta x) \cos(k_z \Delta x)) - 64 \end{aligned} \right] \quad (13) \end{aligned}$$

$$\begin{aligned} & \Gamma(k)_{SO-D3Q27} \\ &= \frac{1}{11(\Delta x)^2} \left[\begin{aligned} & 6(\cos(k_x \Delta x) + \cos(k_y \Delta x) + \cos(k_z \Delta x)) \\ & + 6 \left(\begin{aligned} & \cos(k_x \Delta x) \cos(k_y \Delta x) + \cos(k_x \Delta x) \cos(k_z \Delta x) \\ & + \cos(k_y \Delta x) \cos(k_z \Delta x) \end{aligned} \right) \\ & + 4(\cos(k_x \Delta x) \cos(k_y \Delta x) \cos(k_z \Delta x)) - 40 \end{aligned} \right] \quad (14) \end{aligned}$$

The Fourier modes have been derived in equations (9) – (14) of the discretized 3D Laplacians schemes (4) – (8). These have applications in various physical domains, for example, cell dynamics simulations, Lattice Boltzmann simulations and 3D heat diffusion equations. Then, these schemes, through their Fourier analysis, are combined with the time step value to get better isotropic results in simulations.

5. Isotropy Analysis

In this section, the comparison of isotropy is presented. The isotropy is compared with ideal $-k^2$. The surface contour plots are presented for each Laplacian in the (k_x, k_y) plane to show the quantification isotropy for different schemes where completely circular contours show isotropy of the scheme. The deviation which is like a square-shaped shows anisotropic behaviour. To clearly analyse the isotropic behaviour of Laplacians can compared with the surface contour plot of $-k^2$ which is presented as ideal isotropy condition as a benchmark, shown in Figure 2, The directional bias can be understood from the deviation of contours from circular shape.

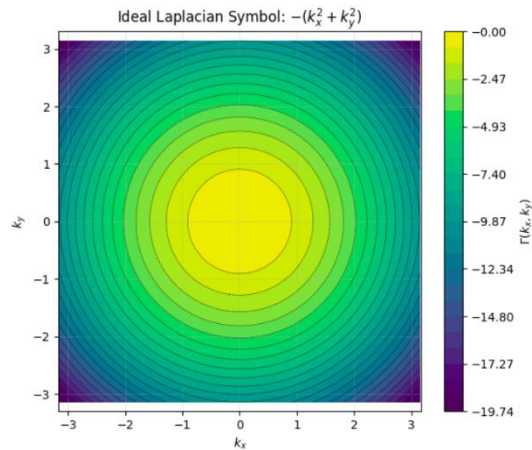


Figure 2. Surface Contour Plot of ideal $-k^2$.

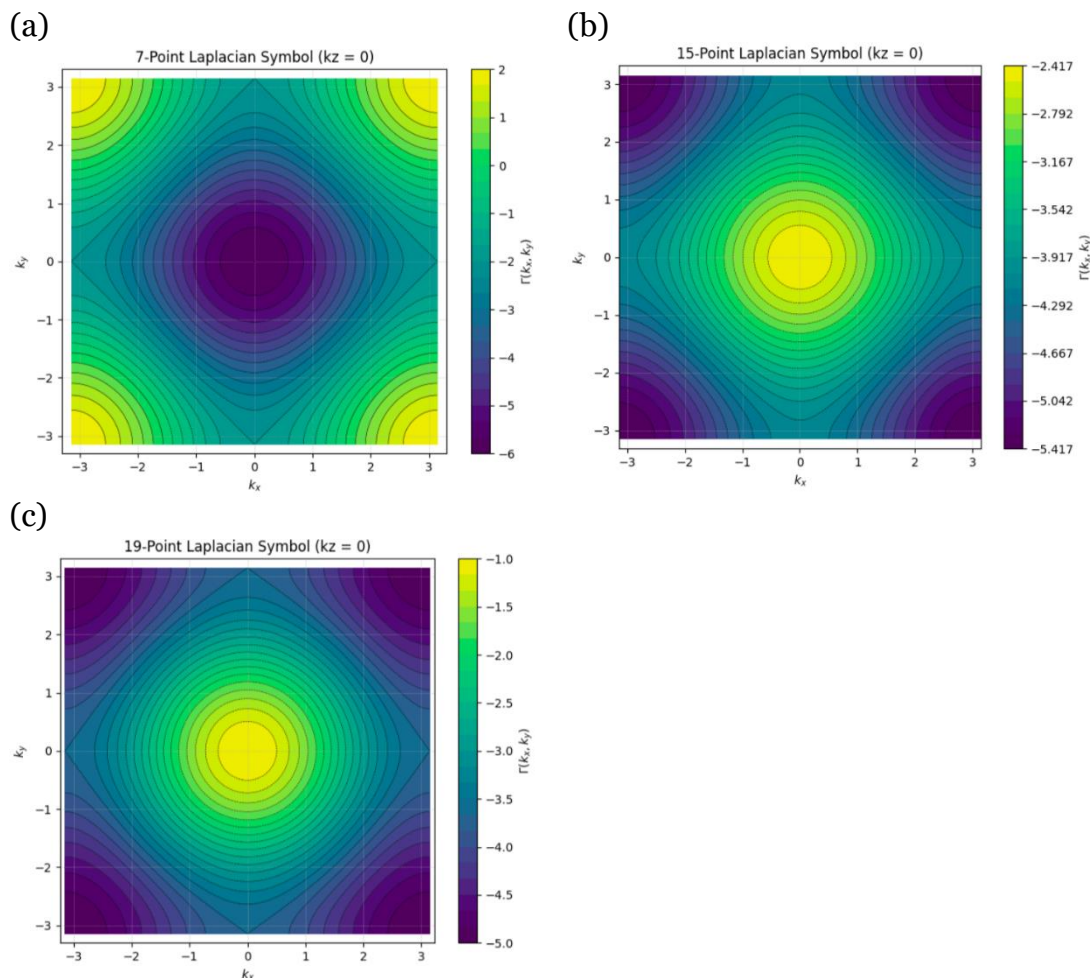


Figure 3. Surface contour plots of 7-point, 15-point and 19-point Laplacians are given in (a), (b) and (c) respectively.

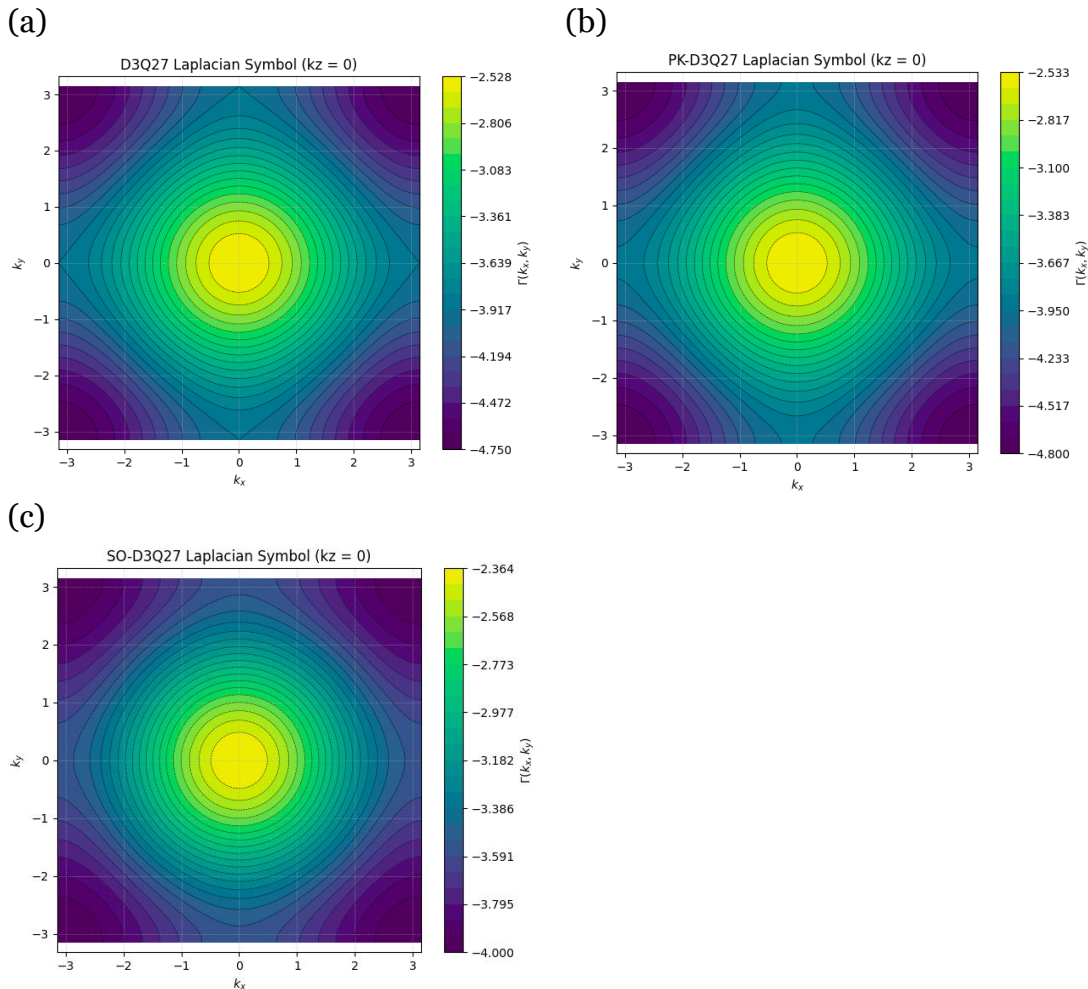


Figure 4. Surface contour plots of 25-point ($D3Q27$), 3D PK and 3D SO Laplacians are given in (a), (b) and (c) respectively.

The surface contour plots based on the Fourier modes are presented to show a suitable method to quantify the isotropy of different discrete 3D Laplacians. The plot of 7-point Laplacian ($D3Q7$), given in Figure 3 (a), shows anisotropy observed from deviation of contours from the ideal circular shapes which results in a directionally biased behaviour. An improved isotropy can be observed in the plots of 15-point ($D3Q15$) and 19-point ($D3Q19$) Laplacians given in Figure 3 (b) and (c) respectively. These both schemes form circular contours near the origin which clearly show their isotropic behaviour. On the other hand, the larger stencils which include a family of 27-point Laplacians show much improved and enhanced isotropy. In all comparisons, the contour plot given in Figure 4 (c) for the Laplacian scheme $SO - D3Q27$ closely matches the ideal Laplacian given in Figure 2. This scheme confirms the directional uniformity. The discrete Laplacians derived for larger stencils especially involving 27 points are more preferred to be used in simulations as isotropic for better accuracy and efficiency.



6. Conclusions

Our work presents a rigorous investigation of different three-dimensional discretised Laplacian operators which include 7-point, 15-point, 19-point and 27-point schemes. All the Laplacians in this work were analysed thoroughly and in perspective of isotropy and stability. The main objective of our work is to investigate the suitability of Laplacians to be utilized in numerical simulations. The simulations which comprise lattice Boltzmann methods, cell-dynamical systems (CDS) and other grid-based solvers are sensitive to directional discretization errors.

The stability analysis was implemented and each Laplacian has been visualized using corresponding Fourier equation. The contour plots on $k_z = 0$ proved to be a quantitative visual tool to measure isotropy. From visualizations, the basic 3D 7-point Laplacian is identified as anisotropic with strong artifacts exhibiting square-shaped contours. The 3D 15-point and 19-point which engage next-nearest neighbours (diagonal neighbours) show improved isotropy, yet deviations of contours compared to ideal contours still exist.

The 3D Laplacians in family of extended 27-point stencils have shown much better isotropy giving closest match with contours of ideal Laplacian. Among all 27-point stencil based Laplacians investigated, the $SO - D3Q27$ has shown the optimal isotropy exhibiting a rotational symmetry making it a perfect choice among 3D Laplacian for simulations. Such isotropic 3D Laplacians has applications in lattice hydrodynamics and CDS models for the simulations of phase separation, pattern formation process and diffusion.

Future work may include extending this analysis to adaptive grids or irregular domains and exploring the impact of these operators on non-linear dynamics and coupled PDE systems.

References

- [1] A. Shinozaki and Y. Oono, "Spinodal decomposition in 3-space," *Phys. Rev. E*, vol. 48, no. 4, pp. 2622–2654, Oct. 1993, doi: 10.1103/PhysRevE.48.2622.
- [2] R. J. LeVeque, *Finite Difference Methods for Ordinary and Partial Differential Equations: Steady-State and Time-Dependent Problems*. Society for Industrial and Applied Mathematics, 2007. doi: 10.1137/1.9780898717839.
- [3] J. C. Strikwerda, *Finite Difference Schemes and Partial Differential Equations, Second Edition*. Society for Industrial and Applied Mathematics, 2004. doi: 10.1137/1.9780898717938.
- [4] M. Patra and M. Karttunen, "Stencils with isotropic discretization error for differential operators," *Numer. Methods Partial Differ. Equ.*, vol. 22, no. 4, pp. 936–953, Jul. 2006, doi: 10.1002/num.20129.
- [5] Y. Oono and S. Puri, "Study of phase-separation dynamics by use of cell dynamical systems. I. Modeling," *Phys. Rev. A*, vol. 38, no. 1, pp. 434–453, Jul. 1988, doi: 10.1103/PhysRevA.38.434.
- [6] F. Family, "Dynamic scaling and phase transitions in interface growth," *Phys. Stat. Mech. Its Appl.*, vol. 168, no. 1, pp. 561–580, 1990.
- [7] J. Weickert, *Anisotropic diffusion in image processing*, vol. 1. Teubner Stuttgart, 1998.
- [8] R. Hahn, *Pierre Simon Laplace, 1749-1827: a determined scientist*. Harvard University Press, 2005.
- [9] G. Patané, "An introduction to laplacian spectral distances and kernels: theory, computation, and applications," in *ACM SIGGRAPH 2017 Courses*, Los Angeles California: ACM, Jul. 2017, pp. 1–54. doi: 10.1145/3084873.3084919.
- [10] G. D. Smith, *Numerical solution of partial differential equations: finite difference methods*. Oxford university press, 1985.



Vol. 3 No. 6 (June) (2025)

- [11] N. W. Ashcroft and N. D. Mermin, "Solid state physics (brooks cole, 1976)," *Cited On*, vol. 26, p. 44, 1993.
- [12] S. Dey and R. Mittra, "A locally conformal finite-difference time-domain (FDTD) algorithm for modeling three-dimensional perfectly conducting objects," *IEEE Microw. Guid. Wave Lett.*, vol. 7, no. 9, pp. 273–275, 1997.
- [13] A. Taflove, S. C. Hagness, and M. Picket-May, "Computational electromagnetics: the finite-difference time-domain method," *Electr. Eng. Handb.*, vol. 3, no. 629–670, p. 15, 2005.
- [14] M. N. Sadiku, *Numerical techniques in electromagnetics*. CRC press, 2000.
- [15] J. H. Ferziger, M. Perić, and R. L. Street, *Computational methods for fluid dynamics*. springer, 2019.
- [16] L.-Q. Chen, "Phase-Field Models for Microstructure Evolution," *Annu. Rev. Mater. Res.*, vol. 32, no. 1, pp. 113–140, Aug. 2002, doi: 10.1146/annurev.matsci.32.112001.132041.
- [17] A. Shinozaki and Y. Oono, "Spinodal decomposition in a Hele-Shaw cell," *Phys. Rev. A*, vol. 45, no. 4, pp. R2161–R2164, Feb. 1992, doi: 10.1103/PhysRevA.45.R2161.
- [18] B. Jähne, *Digital image processing*. Springer Science & Business Media, 2005.
- [19] N. J. Tustison and B. B. Avants, "Explicit B-spline regularization in diffeomorphic image registration," *Front. Neuroinformatics*, vol. 7, p. 39, 2013.
- [20] J. Weickert, *Anisotropic diffusion in image processing*, vol. 1. Teubner Stuttgart, 1998.
- [21] F. Natterer, *The Mathematics of Computerized Tomography*. Society for Industrial and Applied Mathematics, 2001. doi: 10.1137/1.9780898719284.
- [22] J. Virieux, "P-SV wave propagation in heterogeneous media: Velocity-stress finite-difference method," *GEOPHYSICS*, vol. 51, no. 4, pp. 889–901, Apr. 1986, doi: 10.1190/1.1442147.
- [23] D. S. Tuch, "Q-ball imaging," *Magn. Reson. Med.*, vol. 52, no. 6, pp. 1358–1372, Dec. 2004, doi: 10.1002/mrm.20279.
- [24] S. P. Thampi, S. Ansumali, R. Adhikari, and S. Succi, "Isotropic discrete Laplacian operators from lattice hydrodynamics," *J. Comput. Phys.*, vol. 234, pp. 1–7, 2013.
- [25] L.-Q. Chen, "Phase-Field Models for Microstructure Evolution," *Annu. Rev. Mater. Res.*, vol. 32, no. 1, pp. 113–140, Aug. 2002, doi: 10.1146/annurev.matsci.32.112001.132041.
- [26] S. Succi, *The lattice Boltzmann equation: for fluid dynamics and beyond*. Oxford university press, 2001.
- [27] J.-P. Berrut and L. N. Trefethen, "Barycentric Lagrange Interpolation," *SIAM Rev.*, vol. 46, no. 3, pp. 501–517, Jan. 2004, doi: 10.1137/S0036144502417715.
- [28] S. P. Thampi, S. Ansumali, R. Adhikari, and S. Succi, "Isotropic discrete Laplacian operators from lattice hydrodynamics," *J. Comput. Phys.*, vol. 234, pp. 1–7, 2013.
- [29] I. W. Hamley, "Cell dynamics simulations of block copolymers," *Macromol. Theory Simul.*, vol. 9, no. 7, pp. 363–380, Aug. 2000, doi: 10.1002/1521-3919(20000801)9:7<363::AID-MATS363>3.0.CO;2-7.